

## Nuclear symmetry energy and neutron skins derived from pygmy dipole resonances

A. Klimkiewicz,<sup>1,2</sup> N. Paar,<sup>3</sup> P. Adrich,<sup>1,2</sup> M. Fallot,<sup>1</sup> K. Boretzky,<sup>1</sup> T. Aumann,<sup>1</sup> D. Cortina-Gil,<sup>4</sup> U. Datta Pramanik,<sup>1</sup> Th. W. Elze,<sup>5</sup> H. Emling,<sup>1</sup> H. Geissel,<sup>1</sup> M. Hellström,<sup>1</sup> K. L. Jones,<sup>1</sup> J. V. Kratz,<sup>6</sup> R. Kulesa,<sup>2</sup> C. Nociforo,<sup>6</sup> R. Palit,<sup>5</sup> H. Simon,<sup>1</sup> G. Surówka,<sup>2</sup> K. Sümmerer,<sup>1</sup> D. Vretenar,<sup>3</sup> and W. Waluś<sup>2</sup>

(LAND Collaboration)

<sup>1</sup>*Gesellschaft für Schwerionenforschung (GSI), D-64291 Darmstadt, Germany*

<sup>2</sup>*Instytut Fizyki, Uniwersytet Jagielloński, PL-30-059 Kraków, Poland*

<sup>3</sup>*Physics Department, Faculty of Science, University of Zagreb, Bijenička 32, 10000 Zagreb, Croatia*

<sup>4</sup>*Universidade de Santiago de Compostela, E-15706 Santiago de Compostela, Spain*

<sup>5</sup>*Institut für Kernphysik, Johann Wolfgang Goethe-Universität, D-60486 Frankfurt am Main, Germany*

<sup>6</sup>*Institut für Kernchemie, Johannes Gutenberg-Universität, D-55099 Mainz, Germany*

(Received 4 April 2007; published 29 November 2007)

By exploiting Coulomb dissociation of high-energy radioactive beams of the neutron-rich nuclei  $^{129-132}\text{Sn}$  and  $^{133,134}\text{Sb}$ , their dipole-strength distributions have been measured. A sizable fraction of “pygmy” dipole strength, energetically located below the giant dipole resonance, is observed in all of these nuclei. A comparison with available pygmy resonance data in stable nuclei ( $^{208}\text{Pb}$  and  $N = 82$  isotones) indicates a trend of strength increasing with the proton-to-neutron asymmetry. On theoretical grounds, employing the RQRPA approach, a one-to-one correlation is found between the pygmy strength and parameters describing the density dependence of the nuclear symmetry energy, and in turn with the thicknesses of the neutron skins. On this basis, by using the experimental pygmy strength, parameters of the nuclear symmetry energy ( $a_4 = 32.0 \pm 1.8$  MeV and  $p_0 = 2.3 \pm 0.8$  MeV/fm<sup>3</sup>) are deduced as well as neutron-skin thicknesses  $R_n - R_p$  of  $0.24 \pm 0.04$  fm for  $^{132}\text{Sn}$  and of  $0.18 \pm 0.035$  fm for  $^{208}\text{Pb}$ , both doubly magic nuclei. Astrophysical implications with regard to neutron stars are briefly addressed.

DOI: [10.1103/PhysRevC.76.051603](https://doi.org/10.1103/PhysRevC.76.051603)

PACS number(s): 24.30.Cz, 25.60.-t, 25.70.De, 27.60.+j

The neutron root-mean-square (rms) radii of nuclei are fundamental quantities which are difficult to measure in a model-free way [1] and are, therefore, known only for few cases and with relatively poor accuracy [2–4]. This fact is particularly cumbersome since neutron rms radii belong to the few laboratory data that can be used to constrain the isospin-asymmetric part of the equation of state of nuclear matter [5–7], which in turn is closely related, e.g., to the radii of such exotic objects as neutron stars. Neutron skins in heavy nuclei and the crust of neutron stars are both built from neutron-rich nuclear matter and one-to-one correlations were drawn between neutron-skin thicknesses in nuclei [8–10] and specific properties of neutron stars. In a recent paper, Piekarewicz [11] pointed out that the experimentally observed “pygmy” dipole ( $E1$ ) strength [12] might play an equivalent role as the neutron rms radius in constraining the nuclear symmetry energy. Excess neutrons forming the skin give rise to pygmy dipole transitions at excitation energies below the giant dipole resonance; to which extent such transitions represent a collective vibration of excess neutrons against an isospin-symmetric core is theoretically under discussion yet [13–16].

Experimental evidence for pygmy dipole resonances (PDR) is still rather scarce. In an earlier paper [12], we reported on low-lying  $E1$  strength observed in the exotic nuclei  $^{130,132}\text{Sn}$  exhausting a few percent of the energy-weighted Thomas-Reiche-Kuhn (TRK) sum rule. Stable  $N = 82$  isotones and  $^{208}\text{Pb}$  investigated in  $(\gamma, \gamma')$  reactions [17–19] display a concentration of dipole strength below the neutron-separation threshold, absorbing, however, a much smaller fraction of the TRK sum rule.

In the first part of this Rapid Communication we present new experimental data for the unstable isotopes  $^{129,131}\text{Sn}$  and  $^{133,134}\text{Sb}$  obtained from the same measurement as in [12] and provide a comparison to the data from the real-photon scattering experiments with stable nuclei. In the second part, supported by calculations within the relativistic Hartree-Bogoliubov (RHB) model and relativistic quasiparticle random phase approximation (RQRPA) model, we focus on constraining parameters describing the symmetry energy  $S(\rho)$  and eventually extract neutron-skin thicknesses in even-even isotopes  $^{130,132}\text{Sn}$  and  $^{208}\text{Pb}$ . We only very briefly describe the experimental approach and data analysis as the procedures are identical to those outlined in [12].

A beam of  $^{238}\text{U}$  ions was accelerated to a kinetic energy of 550 MeV/nucleon in the SIS-18 synchrotron at GSI, Darmstadt, and secondary radioactive ions were produced by fission in a Be target. Fission products with a mass-to-charge ratio around that of  $^{132}\text{Sn}$  were separated in flight from the primary beam and from other reaction products in the fragment separator FRS and were transported to the experimental area hosting the LAND setup. There, incident ions were identified event-by-event by means of energy loss, time-of-flight, and magnetic-rigidity measurements. The projectiles then passed through a  $^{nat}\text{Pb}$  target where the predominant reaction process is that of electromagnetic (“Coulomb”) dipole excitations to states of relatively high excitation energies which subsequently decay by neutron and  $\gamma$ -ray emission. The excitation energy  $E$  of the projectiles was reconstructed in an invariant-mass analysis using the four-momenta measured with nearly full geometrical acceptance and high efficiency for all decay

products, i.e., the heavy residual nucleus, the neutrons, and the  $\gamma$ -rays. For excitation energies  $E$  just above the neutron separation threshold, relevant in the present context, a resolution of  $\sigma_E \approx 1$  MeV is achieved. After applying corrections for instrumental background (deduced from a measurement without target) and after subtracting contributions from nuclear reactions (deduced from a measurement with a carbon target) the energy-differential Coulomb cross sections were obtained. Finally, subtracting small contributions from quadrupole excitations, the Coulomb cross sections could readily be converted into dipole-strength distributions or photoabsorption cross sections by means of the virtual photon method, based on the semiclassical approximation described in [20,21]. Data with sufficient counting statistics could be accumulated for the isotopes  $^{129,130,131,132}\text{Sn}$  and  $^{133,134}\text{Sb}$ .

The main emphasis of the present Rapid Communication is on quantifying the energetically low-lying dipole strength in excess of that of the giant dipole resonance (GDR). In heavy spherical nuclei, the photoabsorption cross section for the GDR can be well described by a single Lorentzian distribution, the parameters of which vary only very smoothly with proton and neutron number. From our previous analysis for  $^{130,132}\text{Sn}$  [12], the parameters of the Lorentzian distribution were found to be consistent with those known from systematics of stable nuclei (see, e.g., [22,23]). We thus chose a Lorentzian parametrization for all the isotopes under consideration (resonance energy  $E_o = 15.5$  MeV, width  $\Gamma = 4.7$  MeV, photoabsorption cross section integrated up to 25 MeV  $\sigma_\gamma = 2150 \pm 140$  mb MeV). Finally, the parametrized GDR strength distribution was convoluted with the detector response function and subtracted from the experimental distribution. Figure 1 displays the remaining dipole strengths and Table I lists the corresponding integrated values.

As can be seen from Fig. 1, additional low-lying strength appears in all isotopes studied. Distributions for isotopes with odd neutron numbers seem to extend toward lower excitation energies. It should be noted, however, that the experimental data cover excitation energies only above the one-neutron separation energy  $S_n$ , which is significantly higher in case of even neutron numbers in comparison to odd neutron numbers, see Table I.

Figure 2 contrasts the present results with experimental data obtained on stable nuclei available from the literature.

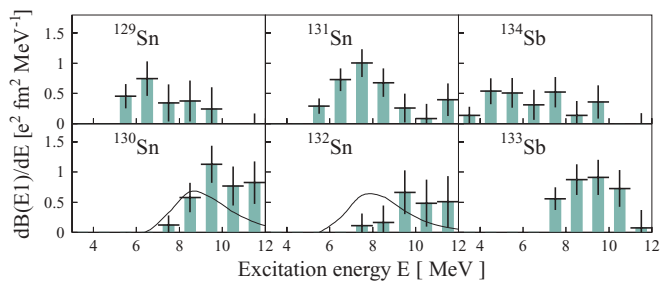


FIG. 1. (Color online) Pygmy dipole strength distribution  $dB(E1)/dE$  obtained for unstable Sn and Sb isotopes with odd-neutron number (upper row) and with even-neutron number (bottom row). The solid lines show results for  $^{130,132}\text{Sn}$  from the RQRPA calculation with a particular choice of the DD-ME interaction, see text.

TABLE I. Neutron separation energies,  $S_n$  [MeV], and  $B(E1)$  [ $e^2\text{fm}^2$ ] values integrated from  $S_n$  up to 11 MeV.

	$^{129}\text{Sn}$	$^{130}\text{Sn}$	$^{131}\text{Sn}$	$^{132}\text{Sn}$	$^{133}\text{Sb}$	$^{134}\text{Sb}$
$S_n$	5.4	7.7	5.2	7.3	7.3	3.3
$B(E1)$	1.7(10)	2.4(7)	3.0(8)	1.3(8)	2.9(9)	2.1(10)

Pygmy dipole-strength data are reported for stable  $N = 82$  isotones [17,18], for  $^{116,124}\text{Sn}$  [24] and for  $^{208}\text{Pb}$  [19]. These stable nuclei were investigated using  $(\gamma, \gamma')$  reactions and  $B(E1)$  distributions were extracted for excited states below the one-neutron separation energy. A number of such measurements reported on the observation of pygmy dipole strength at excitation energies in the interval from 5 to 9 MeV. The  $E1$  distributions for these nuclei above the one-neutron separation threshold which can be derived from experimental photoneutron cross sections (see the data compilation provided in [22]), however, show no evidence for additional pygmy strength. The photoneutron cross sections are almost perfectly fitted by a single Lorentzian distribution. The data for stable nuclei shown in Fig. 2 can thus be considered as the full pygmy dipole strength. Since the one-neutron separation energies for the isotopes of odd neutron number investigated here are rather low, around 5 MeV or below, the derived pygmy strength can be directly compared to that of the stable nuclei. In case of the unstable nuclei with even neutron number ( $^{130,132}\text{Sn}$ ,  $^{133}\text{Sb}$ ) having a higher neutron separation energy, the low-energy part of the pygmy strength might be missed. Nevertheless, Fig. 2 exhibits a clear trend of pygmy dipole strength increasing with the neutron-proton asymmetry  $\alpha = (N - Z)/A$ ; actually, the data are plotted as a function of  $\alpha^2$  that governs the symmetry energy in finite nuclei, see Eq. (1) below. The appearance of a sizable pygmy strength only above a certain value of  $\alpha$  may be not unexpected. The Coulomb force counteracts to some extent the driving force of the symmetry energy toward formation of a neutron skin to which the pygmy strength is related, see the discussion below.

Inspired by this observation, we now turn to the issue of the relation between observed pygmy strength and the symmetry energy in the nuclear equation of state. The PDR is related to a neutron excess giving rise to a neutron skin. It is well un-

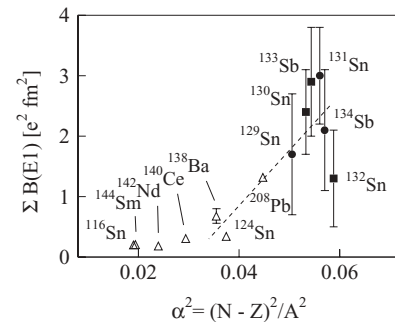


FIG. 2. Pygmy dipole strength from this experiment for unstable  $^{129,130,131,132}\text{Sn}$  and  $^{133,134}\text{Sb}$  nuclei (solid symbols) in comparison with data (open symbols) available for stable nuclei [17–19,24]. The dashed line serves to guide the eye.

derstood that the formation of the neutron skin is governed by the density dependence of the nuclear symmetry energy [5–7]. Using the lowest terms in a Taylor expansion of the energy per nucleon in asymmetric nuclear matter in terms of the density  $\rho$  and the asymmetry parameter  $\alpha = (N - Z)/A$  we obtain

$$E(\rho, \alpha) = E(\rho, 0) + S_2(\rho)\alpha^2 + \dots \quad (1)$$

with the symmetry energy term  $S_2$  parametrized by

$$S_2(\rho) = a_4 + \frac{p_o}{\rho_o^2}(\rho - \rho_o) + \dots, \quad (2)$$

where  $\rho_o$  denotes the saturation density. Evidently,  $a_4$  is equivalent to the symmetry energy in pure neutron matter and  $p_o$  to the symmetry energy pressure, both at saturation density. In various relativistic and nonrelativistic mean-field model parametrizations, the neutron-skin thickness for a given nucleus is practically linearly correlated with both  $a_4$  and  $p_o$  [6,25]; thus the two parameters are strongly correlated with each other. The various mean-field calculations nevertheless may result in very different neutron skins for a particular nucleus, e.g.,  $^{208}\text{Pb}$ . In the following we will show that a given class of mean-field calculations reveal as well a practically linear correlation between the pygmy strength and the neutron-skin thickness in a given nucleus, and thus, also with the symmetry energy parameters.

For this purpose, we have carried out a series of fully self-consistent RHB model [26] plus RQRPA [14] calculations of ground-state properties and dipole strength distributions. A set of density-dependent meson-exchange (DD-ME) effective interactions [27] has been used, for which the parameter  $a_4$  is systematically varied in the interval  $30 \text{ MeV} \leq a_4 \leq 38 \text{ MeV}$  in steps of 2 MeV, while the remaining parameters are adjusted to accurately reproduce nuclear matter properties (the binding energy, the saturation density, the compression modulus, and the volume asymmetry) and the binding energies and charge radii of a standard set of spherical nuclei [27]. For open-shell nuclei, pairing correlations are also included in the RHB+RQRPA framework and described by the pairing part of the Gogny force. The consistent calculation of ground-state properties and dipole strength distributions, using the same effective interaction, provides a direct relation between symmetry energy parameters and the predicted size of the neutron skin and the pygmy strength such as shown for  $^{130,132}\text{Sn}$  in Fig. 3.

In a first step, we inspected the correlation of the neutron-skin thickness in  $^{208}\text{Pb}$  with the  $a_4$  and  $p_o$  parameters, the latter extracted from the density dependence of the symmetry energy around saturation density. We observe an almost linear correlation in both cases and, moreover, these correlations perfectly match the systematics from other mean-field calculations shown in Figs. 7 and 11 of [6].

In a second step, the calculated  $B(E1)$  distributions for  $^{130,132}\text{Sn}$  resulting from the different DD-ME parametrizations were analyzed. In all cases, strength accumulations are found below and clearly separated from the GDR spanning up to 11 MeV excitation energy. The structure of the low-lying states exhibits quite a substantial degree of collectivity due to transitions which involve mainly neutrons from weakly bound orbits. In particular, from the RQRPA calculations for  $^{132}\text{Sn}$  we

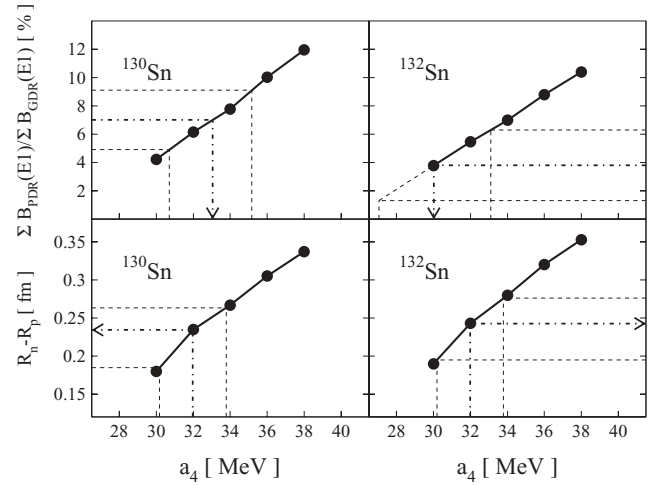


FIG. 3. Upper panels: Ratio of PDR to GDR strength for  $^{130,132}\text{Sn}$  versus the symmetry-energy parameter  $a_4$  as resulting from RQRPA calculations (solid lines). The dot-dashed and dashed lines indicate the experimental PDR/GDR strength ratios with their errors and the range of  $a_4$  values deduced from them. Bottom panels: Neutron-skin thickness  $R_n - R_p$  versus  $a_4$  from RQRPA calculations. The dot-dashed and dashed lines indicate the average  $a_4$  value and its errors and the neutron-skin thicknesses deduced from it.

observe for the two largest states at 7.75 MeV and 8.59 MeV that 10 and 13 neutron transitions contribute with more than 0.1% to the total RQRPA amplitudes, respectively. In the case of  $^{130}\text{Sn}$ , the collectivity of the low-energy states becomes enhanced further more due to the opening of the neutron shell and the increased number of two-quasiparticle configurations which contribute to the low-lying states. For the relevant states at 7.97 MeV and 8.79 MeV, in total 15 and 32 neutron two-quasiparticle configurations participate, respectively, with more than 0.1% in the RQRPA amplitudes. In the case of both Sn isotopes, for each low-energy state the share of neutron transitions amounts to at least 90% of the RQRPA amplitudes while proton transitions contribute to 3–10% only.

In Fig. 1, the  $B(E1)$  strength calculated with the particular choice of  $a_4 = 32$  MeV is convoluted with the detector response function and then compared with the experimental data. The centroid of the calculated distribution is shifted by about one MeV compared to the measured one. In Fig. 3 (upper panels), the calculated  $B(E1)$  strength is integrated up to 11 MeV and, divided by that of the GDR, is shown as a function of  $a_4$ . By comparing the experimental values of the  $B(E1)$  ratio with that of the RQRPA calculations, the symmetry energy parameters were fixed. An average value of  $\bar{a}_4 = 32.0 \pm 1.8$  MeV was obtained from the  $^{130,132}\text{Sn}$  analysis, which is in good agreement with considerations presented in [27]. From the  $a_4$  versus  $p_o$  correlation revealed in the RQRPA calculation, see above, we deduced  $\bar{p}_o = 2.3 \pm 0.8 \text{ MeV/fm}^3$ . The results for  $\bar{a}_4$  and  $\bar{p}_o$  can be confirmed by performing similar RQRPA calculations for  $^{208}\text{Pb}$  and comparing them with the ratio of PDR strength measured in [19] to the GDR strength from [28]; the value  $a_4 = 31$  MeV deduced from these  $^{208}\text{Pb}$  data is consistent with the one obtained for the Sn isotopes.

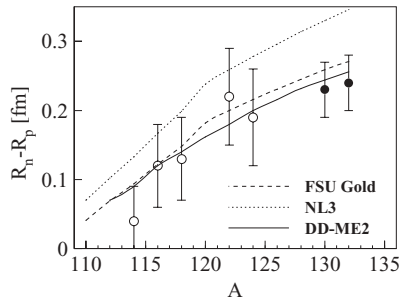


FIG. 4. Neutron-skin thickness in Sn isotopes. The data for stable isotopes (open circles) from [4] are compared to values for  $^{130,132}\text{Sn}$  (filled circles) from this work. Results from different relativistic mean-field calculations available from literature [11,29] are shown as lines.

Finally, using the above average  $\bar{a}_4$  value, neutron-skin thicknesses of  $0.23 \pm 0.04$  fm and of  $0.24 \pm 0.04$  fm for  $^{130}\text{Sn}$  and  $^{132}\text{Sn}$ , respectively, were derived, see bottom panels in Fig. 3. As shown in Fig. 4, these values follow a trend established by a measurement of the stable Sn isotopes [4]. The same procedure applied to the  $^{208}\text{Pb}$  nucleus gives a neutron-skin thickness of  $R_n - R_p = 0.18 \pm 0.035$  fm for  $^{208}\text{Pb}$  in accord with independent measurements which, however, scatter widely [3]. A neutron-skin thickness in  $^{208}\text{Pb}$  of 0.17 fm was deduced from a new analysis of proton elastic scattering data in Ref. [31].

Since the neutron skins in heavy nuclei and the crust of a neutron star are both built from neutron-rich matter, frequently “data-to-data” relations between skin thicknesses, e.g., that of  $^{208}\text{Pb}$  or  $^{132}\text{Sn}$ , and neutron star properties are discussed in the literature. Neutron star properties such as their radii, the transition density  $\rho_c$  from the solid crust to the liquid interior,

or the equilibrium proton fraction as function of baryon density are linked to the neutron skin in nuclei. A detailed analysis of this aspect goes beyond the scope of the present paper. We note, however, that our analysis for  $^{208}\text{Pb}$  favors the “small neutron-skin” option of [9] which excludes a direct URCA process and calls for exotic states of matter to provide enhanced cooling of neutron stars. As another example, an almost linear correlation between the critical transition density  $\rho_c$  in a neutron star and  $R_n - R_p$  in  $^{208}\text{Pb}$  is shown in Fig. 1 of Ref. [8]. Using this relation, from our value deduced above for the neutron skin in  $^{208}\text{Pb}$  one obtains  $\rho_c \approx 0.09 \text{ fm}^{-3}$ . This context shows that PDR-strength distributions measured in the laboratory may help understanding the physics of exotic objects in the universe.

In summary, experimental data on pygmy dipole strength distributions exhibit a correlation with the degree of neutron-proton asymmetry in nuclei. Comparing the measured strength to that obtained within a relativistic mean-field approach, parameters describing therein the nuclear symmetry energy can be constrained and, in turn, neutron-skin thicknesses can be deduced. We are aware that further systematic microscopic model calculations are required in order to confirm as a model-independent trend the correlations between pygmy strength and symmetry energy found in the present calculations. If established, measurements as the ones presented here would provide a precise tool to assess the isospin dependence of the nuclear equation of state.

This work was supported by the German Federal Minister for Education and Research (BMBF) under Contract No. 06MZ174, by the Polish Committee of Scientific Research under Contract No. 1 P03B 001 27, and by the Croatian Ministry of Science and Education under project no. 1191005-1010.

- [1] A. E. L. Dieperink, Y. Dewulf, D. VanNeck, M. Waroquier, and V. Rodin, *Phys. Rev. C* **68**, 064307 (2003).  
 [2] Y. Suzuki *et al.*, *Nucl. Phys.* **A630**, 661 (1998).  
 [3] A. Krasznahorkay *et al.*, *Nucl. Phys.* **A567**, 521 (1994).  
 [4] A. Krasznahorkay *et al.*, *Phys. Rev. Lett.* **82**, 3216 (1999).  
 [5] S. Typel and B. A. Brown, *Phys. Rev. C* **64**, 027302 (2001).  
 [6] R. J. Furnstahl, *Nucl. Phys.* **A706**, 85 (2002).  
 [7] S. Yoshida and H. Sagawa, *Phys. Rev. C* **69**, 024318 (2004).  
 [8] C. J. Horowitz and J. Piekarewicz, *Phys. Rev. Lett.* **86**, 5647 (2001).  
 [9] C. J. Horowitz and J. Piekarewicz, *Phys. Rev. C* **66**, 055803 (2002).  
 [10] A. W. Steiner *et al.*, *Phys. Rep.* **441**, 325 (2005).  
 [11] J. Piekarewicz, *Phys. Rev. C* **73**, 044325 (2006).  
 [12] P. Adrich *et al.*, *Phys. Rev. Lett.* **95**, 132501 (2005).  
 [13] D. Vretenar, N. Paar, P. Ring, and G. A. Lalazissis, *Nucl. Phys.* **A692**, 496 (2001).  
 [14] N. Paar, P. Ring, T. Nikšić, and D. Vretenar, *Phys. Rev. C* **67**, 34312 (2003).  
 [15] D. Sarchi, P. F. Bortignon, and G. Colò, *Phys. Lett.* **B601**, 27 (2004).  
 [16] N. Tsoneva, H. Lenske, and C. Stoyanov, *Phys. Lett.* **B586**, 213 (2004).  
 [17] A. Zilges *et al.*, *Phys. Lett.* **B542**, 43 (2002).  
 [18] S. Volz *et al.*, *Nucl. Phys.* **A779**, 1 (2006).  
 [19] N. Ryezayeva *et al.*, *Phys. Rev. Lett.* **89**, 272502 (2002).  
 [20] A. Winther and K. Alder, *Nucl. Phys.* **A319**, 518 (1979).  
 [21] C. A. Bertulani and G. Baur, *Phys. Rep.* **163**, 299 (1988).  
 [22] S. S. Dietrich and B. L. Berman, *At. Data Nucl. Data Tables* **38**, 200 (1988).  
 [23] M. N. Harakeh and A. van der Woude, *Giant Resonances*, Vol. 24 of Oxford Studies in Nuclear Physics (Oxford University Press, Oxford, 2001).  
 [24] K. Govaert *et al.*, *Phys. Rev. C* **57**, 2229 (1998).  
 [25] L. W. Chen, C. M. Ko, and B. A. Li, *Phys. Rev. C* **72**, 064309 (2005).  
 [26] D. Vretenar, A. V. Afanasjev, G. A. Lalazissis, and P. Ring, *Phys. Rep.* **409**, 101 (2005).  
 [27] D. Vretenar, T. Nikšić, and P. Ring, *Phys. Rev. C* **68**, 024310 (2003).  
 [28] A. Veyssiere *et al.*, *Nucl. Phys.* **A159**, 561 (1970).  
 [29] N. Paar *et al.*, *Phys. Lett.* **B606**, 288 (2005).  
 [30] B. C. Clark, L. J. Kerr, and S. Hama, *Phys. Rev. C* **67**, 054605 (2003).  
 [31] S. Karataglidis, K. Amos, B. A. Brown, and P. K. Deb, *Phys. Rev. C* **65**, 044306 (2002).